How to get the yield locus of an adhesive powder from a single numerical experiment

Stefan Luding [1] **and Fernando Alonso-Marroquin** [2]

1 Multi Scale Mechanics, TS, CTW, UTwente,
POBox 217, 7500 AE Enschede, Netherlands;

2 MoSCoS, School of Mathematics and Physics,
The University of Queensland, Sta Lucia, Qld 4108, Australia;

ABSTRACT Granular materials in a split-bottom ring shear cell geometry show wide shear bands under slow, quasi-static deformation. From discrete element simulations (DEM), several continuum fields like the deformation gradient and stress are computed and evaluated with the goal to formulate objective constitutive relations for the flow behavior.
From a single simulation only, by applying time- and (local) space-averaging, yield loci can be obtained: linear for non-cohesive granular materials and non-linear with peculiar pressure dependence for adhesive powders. While the contact model will possibly need additional effects to be included in order to resemble realistic powders, the method how to obtain yield loci from a single numerical test on one material appears very promising and waits for calibration and validation.

1 INTRODUCTION

Granular materials are a paradigm of complex systems, where phenomena like segregation, clustering, shear-band formation and arching occur due to the collective behavior of many particles interacting via contact forces. Discrete Element Models (DEM) allow the specification of particle properties and interaction laws and then the numerical solution of Newton's equations of motion [1, 2]. For geotechnical applications and industrial design in mechanical engineering, one of the main challenges is to obtain continuum constitutive relations and their relevant parameters from experimental and numerical tests on representative samples.
DEM simulations of similar element tests provide advantages with respect to physical experiments, as they provide more detailed information of forces and displacements at the grain scale. Finding the connection between the micromechanical properties and the macroscopic behavior involves the so-called micro-macro transition [3–8]. Extensive "microscopic" simulations of many homogeneous small samples, i.e., so-called representative volume elements (RVE), have been used to derive the macroscopic constitutive relations needed to describe the material within the framework of a continuum theory [3, 5].
An alternative – as presented in this study – is to simulate an inhomogeneous geometry where static packings co-exist with dynamic, flowing zones and, respectively, high density co-exists with dilated zones. From adequate local averaging over equivalent volumes – inside which all particles behave similarly – one can obtain from a single simulation already constitutive relations in a certain parameter range, as was done systematically in two-dimensional (2D) Couette ring shear cells [6, 9] and three-dimensional (3D) split-bottom ring shear cells [8, 10].

The special property of the split-bottom ring shear cell is the fact that the shear band is initiated at the bottom gap between the moving, outer and fixed, inner part of the bottom-wall. The velocity field is well approximated by an error-function [7, 8, 11, 12] with a width considerably increasing from bottom to top (free surface). The data-analysis provides data-sets of different pressures, shear-stresses and shear-rates – from a single simulation only. Previous simulations with dry particles were validated by experimental data and quantitative agreement was found with deviations as small as 10 per-cent [8, 10, 12].
Note that both time- and space-averaging are required to obtain a reasonable statistics. Furthermore, we remark, that even though ring-symmetry and time-continuity are assumed for the averaging, this is not true in general, since the granular material shows non-affine deformations and intermittent behavior. Nevertheless, the time- and space-averages are performed as a first step to obtain continuum quantities – leaving an analysis of their fluctuations to future studies.

2 The Soft Particle Molecular Dynamics Method

The behavior of granular media is simulated with the discrete element method (DEM) or molecular dynamics (MD) [5–7, 13]. Both methods are identical in spirit, however, MD was developed for numerical simulations of atoms and molecules [1], while DEM was introduced by Cundall for modeling geological materials [2]. While MD typically involves pair interaction potentials, the essential ingredient of DEM modelling is the force-displacement relation (which often cannot be related to a potential) that governs the interaction between pairs of particles in normal and tangential direction (as well as for torques, which are not considered here however). Particle positions, velocities and interaction forces are then sufficient to integrate the equations of motion for all particles simultanelously.
Since the exact calculation of the deformations of the particles is computationally too expensive, we assume that the particles can interpenetrate each other. Then we relate the normal interaction force to the overlapping length as $f = k\delta$, with a stiffness k. In the tangential direction, the force $f^t = k_t\delta^t$ is proportional to the tangential displacement of the contact points (due to both rotations and sliding) with a stiffness k_t. The tangential force is limited by Coulomb's law for sliding $f^t \leq \mu f$, i.e., for $\mu = 0$ one has no tangential forces at all. In order to account for energy dissipation, the normal and tangential degrees of freedom are also subject to a viscous, velocity dependent damping force. For more details see [7, 14].
For fine dry particles, not only friction is relevant, but also adhesive contact properties due to van der Waals forces. Furthermore, due to the tiny contact area, even moderate forces can lead to plastic yield and irreversible deformation of the material in the vicinity of the contact. This complex behavior is modeled by introducing a variant of the linear hysteretic spring model, as explained in [7, 8].
The adhesive, plastic (hysteretic) force is introduced by allowing the normal stiffness constant k to depend on the history of the deformation. This involves a higher stiffness for un-loading, which also increases with the previous maximal load. The overlap when the unloading force reaches zero resembles the permanent plastic deformation, and the negative forces reached thereafter are attractive, adhesion forces, which increase non-linearly with the previous maximal compression force experienced. The three physical phenomena elasticity/stiffness, plasticity and adhesion are thus quantified by three material parameters k_2, k_1, and k_c, respectively. Plasticity disappears for $k_1 = k_2$ and adhesion vanishes for $k_c = 0$.
The parameters of the model are: normal stiffness $k_2 = 500\,\mathrm{N/m}$, plastic stiffness $k_1/k_2 = 1/5$, tangential stiffness $k_t/k_2 = 1/25$ The contact friction coefficient is $\mu = 0.01$, the rolling and torsion yield limits are inactive, i.e., $\mu_r = 0.0$ and $\mu_o = 0.0$. The normal and tangential viscosities are $\gamma_n = 0.002\,\mathrm{s}^{-1}$ and $\gamma_t = 0.0005\,\mathrm{s}^{-1}$, and the density is $\rho = 2000\,\mathrm{kg/m}^3$.

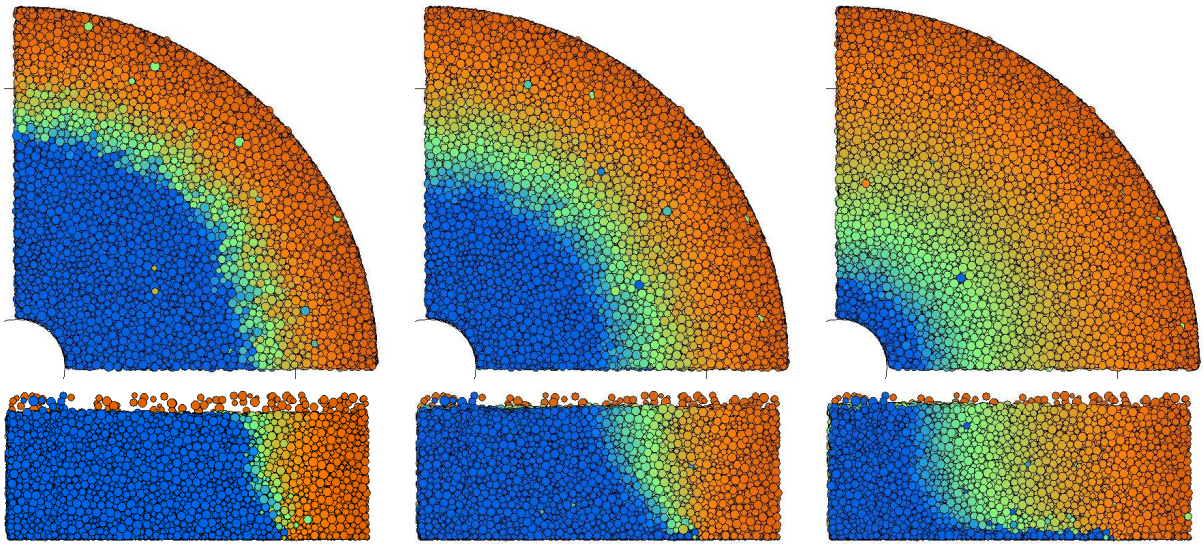

Figure 1: Snapshots from simulations with different adhesion constants, but the same number of mobile particles $N = 34518$, seen from the top and from the front. The material is without cohesion $k_c/k_2 = 0$ (Left) with moderate adhesion, $k_c/k_2 = 2/5$ (Center) with strong adhesion $k_c/k_2 = 1$ (Right). The colors blue, green, orange and red denote particles with displacements in tangential direction per second $r\,\mathrm{d}\phi \leq 0.5\,\mathrm{mm}$, $r\,\mathrm{d}\phi \leq 2\,\mathrm{mm}$, $r\,\mathrm{d}\phi \leq 4\,\mathrm{mm}$, and $r\,\mathrm{d}\phi > 4\,\mathrm{mm}$.

The geometry of the sample is described in detail in Refs. [8, 10]. In brief: An assembly of spherical particles is confined by gravity between two concentric cylinders, a split ring-shaped bottom and a free surface at the top. The outer cylinder rotates around the symmetry-axis and the outer part of the bottom is moving together with it. The split allows that the inner part of the bottom remains at rest and the split initiates the shearband that propagates upwards and becomes wider with increasing height, see Fig. 1.

The simulations run for more than 50 s with a rotation rate $f_o = 0.01\,\mathrm{s}^{-1}$ of the outer cylinder, with angular velocity $\Omega_o = 2\pi f_o$. For the average of the displacement, only larger times are taken into account so that the systems quasi-steady state flow is examined – disregarding the transient behavior at the onset of shear. Three realizations with the same filling height, i.e., $N \approx 37000$ overall particles, are displayed in Fig. 1, both as top- and front-view without ($k_c = 0$) and with adhesion ($k_c/k_2 = 2/5$ and 1). The color code indicates the displacement and shows that without cohesion the shear band is narrower than with cohesion. Furthermore, strong cohesion makes the shearband move rapidly inwards close to the bottom (Right panel).

Since we assume translational invariance in the tangential ϕ-direction, averaging is performed over toroidal volume elements and over many snapshots in time (typically $40 - 60\,\mathrm{s}$), leading to fields $Q(r, z)$ as function of the radial and vertical positions. The averaging procedure was detailed for 2D systems e.g. in Ref. [6], and applied to three dimensional systems [7, 8], so that we do not discuss the details here.

Just examined from the top (like in the original experiments), one observes that the shearband moves inwards with increasing filling height (data not shown) and also becomes wider. The present data show a similar behavior for different contact adhesion: The shearband moves inwards with increasing adhesion stiffness, i.e., with increasing adhesion strength. From the front-view, the same information can be evidenced, see Fig. 1.

Comparing the cases with (Center, Right) and without (Left) adhesion in Fig. 1, the shearband appears to depend strongly on adhesion. In order to allow for a more quantitative analysis of the shear band, both on the top and as function of depth, fits with the universal shape function

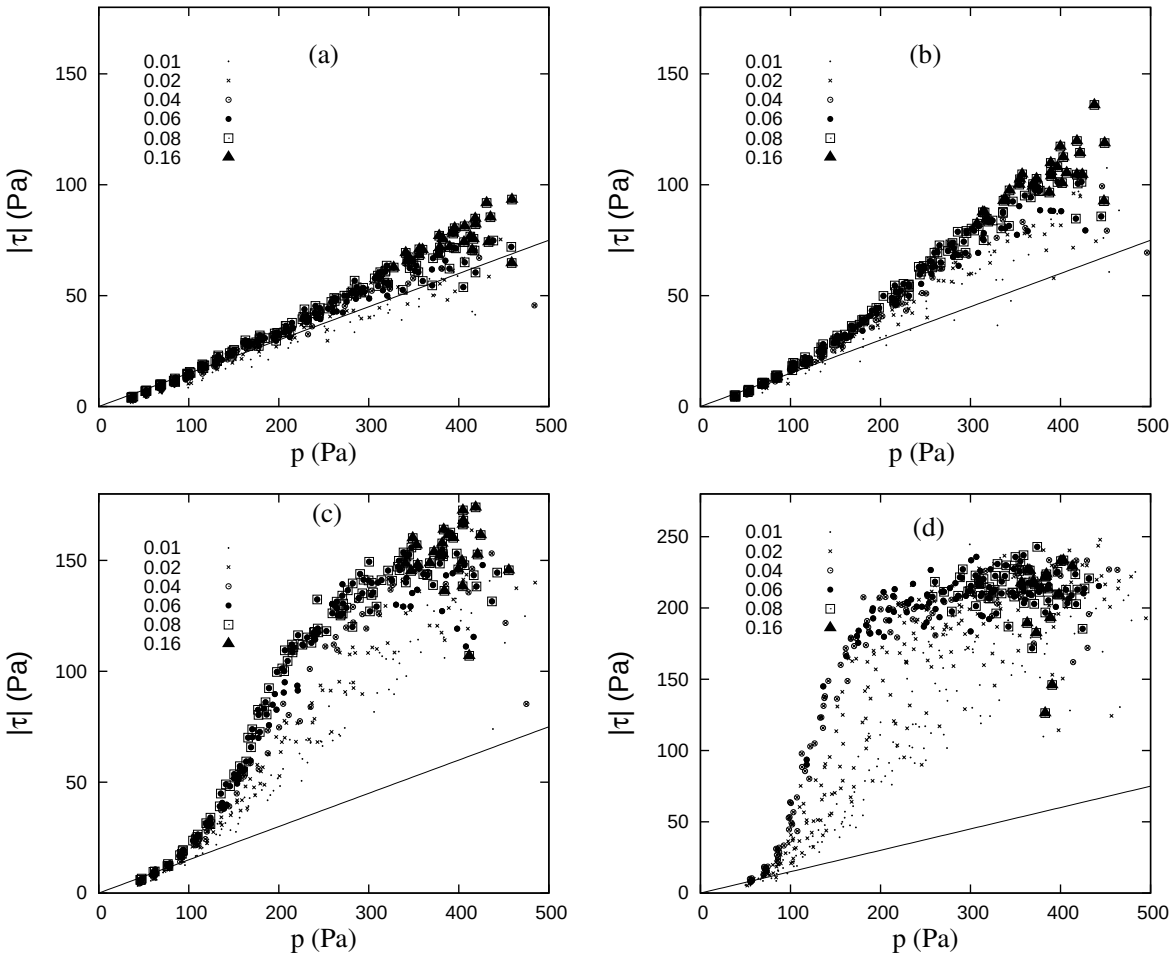

Figure 2: Shear stress $|\tau|$ plotted against pressure p for three different adhesive parameters: $k_c/k_2 = 0$ (a), $k_c/k_2 = 1/10$ (b), $k_c/k_2 = 1/5$ (c) and $k_c/k_2 = 2/5$ (d). The magnitude of the strain rate, i.e., $\dot{\gamma} \geq \dot{\gamma}_i$, with $\dot{\gamma}_i$ are given in the inset in units of s^{-1}. The solid line represents the function $\tau_{\max} = \mu^{macro} p$, where $\mu^{macro} = 0.15$ was used here.

proposed in Ref. [15] can be performed, see Ref. [8].

A quantitative study of the averaged velocity field, and the velocity gradient derived from it, leads to the definition of the local strain rate, $\dot{\gamma} = \sqrt{\left(\partial v_\phi/\partial r - v_\phi/r\right)^2 + \left(\partial v_\phi/\partial z\right)^2}/2$, i.e., the shear intensity in the shear plane, as discussed in Refs. [7, 8].

Furthermore, one can determine the components of the stress tensor as $\sigma_{\alpha\beta} = \frac{1}{V}\sum_{c\in V} f_\alpha l_\beta$, with the components of the contact forces f_α and branch vectors l_β, which connects the center of mass of the particle with the contact point. The sum extends over all contacts within or close to the averaging volume, weighted according to their vicinity – a more detailed description of the averaging procedure and the weighting will be published elsewhere. Note that we disregard the (small) tangential forces here for the sake of simplicity. The shear stress is defined in analogy to the shear strain as proposed in [16], so that: $|\tau| = \sqrt{\sigma_{r\phi}^2 + \sigma_{z\phi}^2}$.

Remarkably, for non-cohesive materials the macroscopic friction $|\tau|/p \approx \mu^{macro}$, is well defined (data not shown, see Refs. [7, 8]), i.e. the slope of the shear stress–pressure curve is almost constant for practically all averaging volumina with strain rates larger than some threshold value. In other words, if the shear length $l_\gamma \approx t_{av}\dot{\gamma}$, with averaging time t_{av}, clearly exceeds one particle diameter, the shear deformation is fully established – resembling the concept of a critical

flow regime. Therefore, for the present data-set, we observe that $\dot{\gamma} > \dot{\gamma}_c$, with $\dot{\gamma}_c \approx 0.12\,\mathrm{s}^{-1}$ is a reasonable shear-rate above which the shear-layers in the shear-band are fully established.
When contact adhesion is included in the model, a non-linear yield locus is obtained with a peculiar pressure dependence. This non-linearity becomes apparent when we plot the shear stress against pressure for different coefficients of adhesion, as shown in Fig. 2. The main effect of contact adhesion is to increase the strength of the material under large confining stress. For weak adhesion the strength is given by an almost linear relation between shear stress and pressure, while the relation is highly non-linear for large adhesion.
The microscopic reason of this nonlinearity is the non-linearity of the contact model: The contacts feel small adhesion forces for small experienced pressure (close to the free surface). Very large adhesion forces are active for high pressures deep in the bulk of the material. Therefore the micromechanical mechanisms involve not only plastic deformation of the contact zone, but also sintering, fragmentation and re-bonding under large stress conditions.

3 Conclusions

Simulations of a split-bottom Couette ring shear cell with dry granular materials show perfect qualitative and good quantitative agreement with experiments. The effect of friction was studied recently, so that in this study the effect of contact adhesion was examined in some detail. The yield locus, i.e., the maximal shear stress, $|\tau|$, plotted against pressure – for those parts of the system that have experienced considerable shear (displacement) – is almost linear in the absence of adhesion, corresponding to a linear Mohr-Coulomb type yield locus with slope (macroscopic friction) increasing with microscopic contact friction.
Strong non-linearity of the yield locus emerges as a consequence of the strong adhesive forces that increase non-linearly with the confining pressure. Due to the non-linearity, the definition of a macroscopic cohesion (as shear stress of the yield locus at zero-stress) becomes questionable. All this interesting phenomenology is due to the history dependent contact model: Contacts that experienced large stresses can provide much larger adhesive forces than others which have not been compressed a lot. Therefore, at the top (free surface) the yield stress is much lower then deep inside the sample.
The physical origin of this nonlinearity is the permanent deformation at the contact which leads to a larger contact surface area and therefore to stronger van der Waals forces. As final remark, we note that the model contains an unphysical simplification: The long range van der Waals adhesion is neglected and only the short range contact adhesion is considered. Future studies with the long range (non-contact) term will show whether this can lead to more linear and cohesive yield locus. In real systems of dry, adhesive powders, the long range adhesion will provide the bulk cohesion, since – as shown in this study – the contact adhesion alone is not effective at small confining pressure.
Future research will also involve the yield locus of materials with different friction, rolling resistance and torsion resistance as well as non-spherically shaped particles.

4 Acknowledgements

We acknowledge the financial support of the Deutsche Forschungsgemeinschaft (DFG), the Stichting voor Fundamenteel Onderzoek der Materie (FOM), financially supported by the Nederlandse Organisatie voor Wetenschappelijk Onderzoek (NWO), the Australian Research Council, the Australian Academy of Sciences, and the University of Queensland Early Carrier Research Grant.

References

[1] M. P. Allen and D. J. Tildesley. *Computer Simulation of Liquids*. Oxford University Press, Oxford, 1987.

[2] P. A. Cundall. A computer model for simulating progressive, large-scale movements in blocky rock systems. In *The International Symposium on rock mechanics*, Nancy, France, 1971.

[3] F. Alonso-Marroquin and H.J. Herrmann. Investigation of the incremental response of soils using a discrete element model. *J. of Eng. Math.*, 52:11–34, 2005.

[4] K. Bagi. Microstructural stress tensor of granular assemblies with volume forces. *J. Appl. Mech.*, 66:934–936, 1999.

[5] P. A. Vermeer, S. Diebels, W. Ehlers, H. J. Herrmann, S. Luding, and E. Ramm, editors. *Continuous and Discontinuous Modelling of Cohesive Frictional Materials*, Berlin, 2001. Springer. Lecture Notes in Physics 568.

[6] M. Lätzel, S. Luding, and H. J. Herrmann. Macroscopic material properties from quasi-static, microscopic simulations of a two-dimensional shear-cell. *Granular Matter*, 2(3):123–135, 2000.

[7] S. Luding. Cohesive frictional powders: Contact models for tension. *Granular Matter*, 10:235–246, 2008.

[8] S. Luding. The effect of friction on wide shear bands. *Particulate Science and Technology*, 26(1):33–42, 2008.

[9] M. Lätzel, S. Luding, H. J. Herrmann, D. W. Howell, and R. P. Behringer. Comparing simulation and experiment of a 2d granular couette shear device. *Eur. Phys. J. E*, 11(4):325–333, 2003.

[10] S. Luding. Constitutive relations for the shear band evolution in granular matter under large strain. *Particuology*, 6(6):501–505, 2008.

[11] D. Fenistein, J. W. van de Meent, and M. van Hecke. Universal and wide shear zones in granular bulk flow. *Phys. Rev. Lett.*, 92:094301, 2004. e-print cond-mat/0310409.

[12] S. Luding. Particulate solids modeling with discrete element methods. In P. Massaci, G. Bonifazi, and S. Serranti, editors, *CHoPS-05 CD Proceedings*, pages 1–10, Tel Aviv, 2006. ORTRA.

[13] S. Luding. Micro-macro transition for anisotropic, frictional granular packings. *Int. J. Sol. Struct.*, 41:5821–5836, 2004.

[14] S. Luding. Collisions & contacts between two particles. In H. J. Herrmann, J.-P. Hovi, and S. Luding, editors, *Physics of dry granular media - NATO ASI Series E350*, page 285, Dordrecht, 1998. Kluwer Academic Publishers.

[15] D. Fenistein and M. van Hecke. Kinematics – wide shear zones in granular bulk flow. *Nature*, 425(6955):256, 2003.

[16] M. Depken, W. van Saarloos, and M. van Hecke. Continuum approach to wide shear zones in quasistatic granular matter. *Phys. Rev. E*, 73:031302, 2006.